

ORIGINAL RESEARCH PAPER

Pages: 231-242

Distributed Targets Modelling using Canonical Shapes in Synthetic Aperture Radar Systems

N. Sadat Vaez¹, M. Behzad Fallahpour^{1*}, H. Dehghani¹, and E. Ghasemi¹

Electrical Engineering dept., Maleke Ashtar University of technology, Tehran, IRAN

nsvaez68@gmail.com, m_behzad_fp@yahoo.com, , hamid_deh@yahoo.com, ghaseme.elham@gmail.com

Corresponding author: m_behzad_fp@yahoo.com

DOI:10.22070/JCE.2023.17616.1240

Abstract- In this paper, in order to simplify calculation of the distributed target response, a new model of distributed targets is presented using monostatic SAR (Synthetic Aperture Radar) imagery. Distributed targets are strategic, because they are important in various fields, especially in military. Calculating the response of these targets is difficult due to the complexity of modelling and scattering data calculation. We solve this problem with replacing the scattered pixels with canonical shapes. Besides the simplicity, this model gives the response close to the real model. This model facilitates the target detection, target design, scattering data analysis, and distributed targets interpretation of radar viewing. In fact, one of the goals of this paper is to predict the scattering data of a scene. For this purpose, the scattering field of a real model is calculated and compared with the proposed model.

Index Terms- SAR, Monostatic, Distributed target imagery, scattered pixels, Canonical shapes.

I. INTRODUCTION

Diagnosing behavioral patterns of the targets in the scene is one of the important challenges of signal processing in image analysis [1]. Modelling and calculating scattering fields are very complicated for some distributed targets. The scattering response of these targets is important. So, designing a simple model is important, because instead of a real target, it gives response close to the real model. The model can aid to design the target, extract features, identify and recognize the target in the scene, interpret and analyses targets [1-3]. Also, the library is usually suggested in this study. Geometric and CAD (Computer-aided design) models are used to study the distributed targets [4-6]. These models are created in various software that cause the complexity of construction and scattering calculations [7]. Due to the complexity of the distributed targets, a simple model is required. Usually, pointing

model is used to solve this problem. The pointing model shows scattering centers. The reflection of these points is the most returns of the target to the radar [8, 9]. Due to the different mechanisms of scattering, only some of the target points are scattered to the radar in the monostatic SAR radars. In fact, the response of mirror reflections at angular surfaces with radar do not return. In distributed targets, the image of the target is only the scattering pixels. Scattering pixels are such as the plate toward the radar, reflector, sphere, corners, and so on. The received data of the target have the target features [10, 11]. The shape parameter and target orientation are important to determine the replacement of scattered pixels [12]. Given that the canonical shapes have been used in the model, it simplifies the creation of the model for large targets. Also, the complexity of scattering calculations reduces by modelling only the scattered pixels.

The SAR software model which is developed in this paper is a tool to present the scattering model of distributed targets using canonical shapes. Therefore, in the second part of this paper, the SAR software model is explained. Next, the proposed algorithm is presented to distributed targets imagery using the SAR radar, and finally, the simulation results are presented and compared with the simulation results of the CAD model.

II. SOFTWARE MODEL OF SAR

Length of SAR radar antenna is virtually manifold the real length of the antenna. Returned echo of a target is stored in different positions of the virtual antenna, and according to the Doppler frequency which is unique for each point of the earth, target's response with high resolution is recorded by Doppler shift frequency and post-processing. After sending each pulse, the result of each echo is received in the receiver and sampled after transferring to the baseband. This sampling is performed in the range direction, and the samples for each echo are placed in a specified row of two-dimensional arrays. As the platform moves from the top of the scene, the pulses are sequentially transmitted, and the rows of this two-dimensional array are filled. This two-dimensional array is called raw data [10, 13]. Since this matrix space does not have the special visual information, image space is obtained for better visualization. The image space is a two-dimensional data, which illustrates the scattered signal from target to the radar in the pixels of the scene.

The SAR simulator presented in [14] is based on SAR imagery and used for distributed target modelling. This software contains three basic steps for acquiring the raw data, forming the signal and the image space as shown in Fig. 1. This simulator is briefly explained in this section.

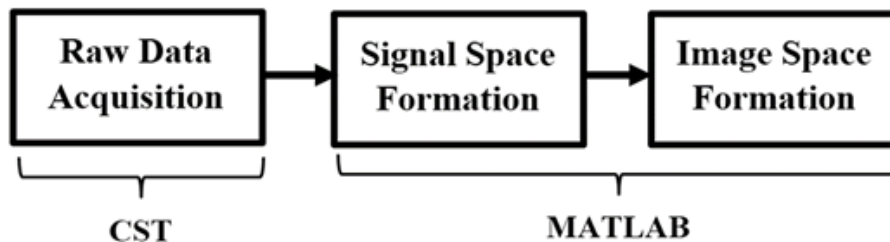


Fig. 1. Software implementation of SAR [14].

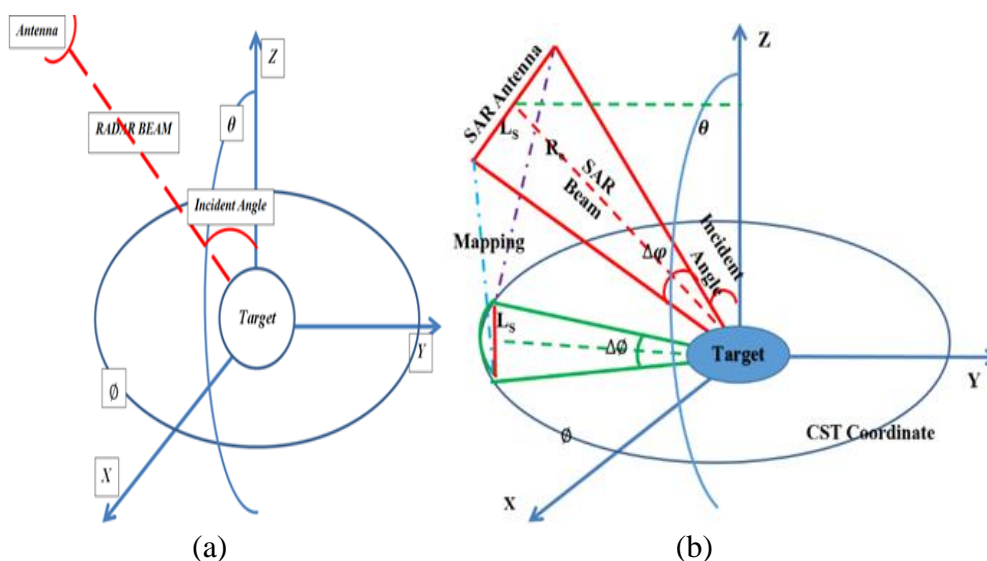




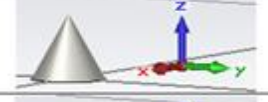



Fig. 2. a) Scanning a target, b) Using CST in the form of SAR from a geometry perspective [14].

The main challenge in using the CST software is the lack of SAR radar. In this software, the radar motion in the azimuth direction and sampling in the range direction are considered in two directions in the spherical coordinates to scan the target. As shown in Fig. 2, θ is scanning in the vertical and ϕ is scanning in the horizontal direction. Incidence angle in SAR defines the angle between the wave path and the line perpendicular to the ground. So, according to Fig. 2 a, the scan in the vertical direction (θ) is considered as an equivalent to incidence angle in SAR. Also, according to Fig. 2 b, scanning in the horizontal direction (ϕ) can be considered as an equivalent to the movement of SAR.

III. DISTRIBUTED TARGET IMAGERY

When electromagnetic waves hit a target, the part of the incident wave is absorbed and the rest is scattered. This scattered wave in the monostatic is a part of the scattered wave of the target, that carrying the target's properties. In SAR radar, many internal and external system parameters affect Radar images, such as radar, platform, processing algorithms, and imaging region, which has several different sub-parameters. In target recognition, the value or amount of the scan ($\Delta\phi$) in the spherical

Table I. Some creatable shapes in the CST software

Target Shape	Target
Cube	
Cylinder	
Cone	
Sphere	
Trihedral	
Dihedral	

coordinates in the CST is important. To obtain this value according to Fig. 2 b, the movement of the SAR in the space (L_s) is mapped to the CST scan value in the spherical coordinate ($\Delta\phi$). Therefore, using CST as the SAR radar is provided [14].

Frequency parameter, polarization, target orientation, and target shape are effective. The polarization and frequency are the radar parameters. These parameters are fixed in presented and reference models. But the orientation and target shape are target parameters that should be considered in modelling [1, 10, 11]. There are two problems in confronting with the distributed targets. Because the complexity of the targets, the first problem is making the model and the second problem is the simulation of distributed models. The proposed model simplifies the modelling and computation of scattering fields with good accuracy. In this model, only scattered pixels are considered and they are replaced by canonical shapes close to the model. Shapes are designed in the CST software easily. Some of these shapes are given in table I.

As mentioned above, in addition to choosing the shape, the orientation of the targets is also important. For example, the dispersion fields for a cylinder are not the same in vertical and the horizontal directions. Also for the cone and other shapes, the orientation of the target affects the results of the fields [15].

The following are four steps used for modelling distributed targets:

1. Identify scattering pixels in distributed target
2. Determine the position, orientation, and target shape in scattering pixels
3. Select the canonical shape close to the target
4. Simulate scattering pixels

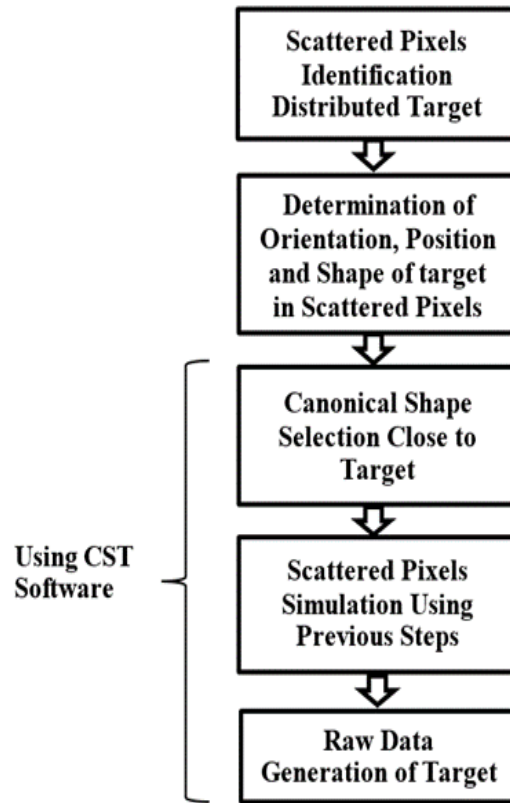


Fig. 3. Implementation of the presented model for distributed targets and raw data generation.



Fig. 4. Steps for image space formation of the presented model.

The first step is the scattering pixels identification such as the plate toward the radar, reflector, sphere and corners. In the second step, the target shape and its orientation, as well as its position (x, y, z) is determined. In the next step, the canonical shape will be selected close to the target shape, then the simulation of the selected shape of the pixels in the position and determined orientation will be done in the CST software, and the target scattering fields using this software will be calculated, and raw data will be generated.

Table II. Characteristics of simulated SAR

Characteristics	Value
Carrier Frequency	$f_c=10$ GHz
Range Resolution	$R_r = 1$ m
Azimuth Resolution	$R_a=1$ m
Polarization	HH
Incidence Angle(deg)	$\theta = 45^\circ$
Scan Angle(deg)	$\varphi = 90^\circ$

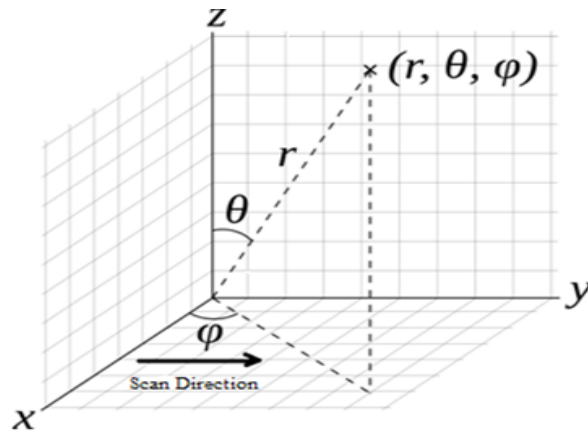


Fig. 5. The imaging coordinates.

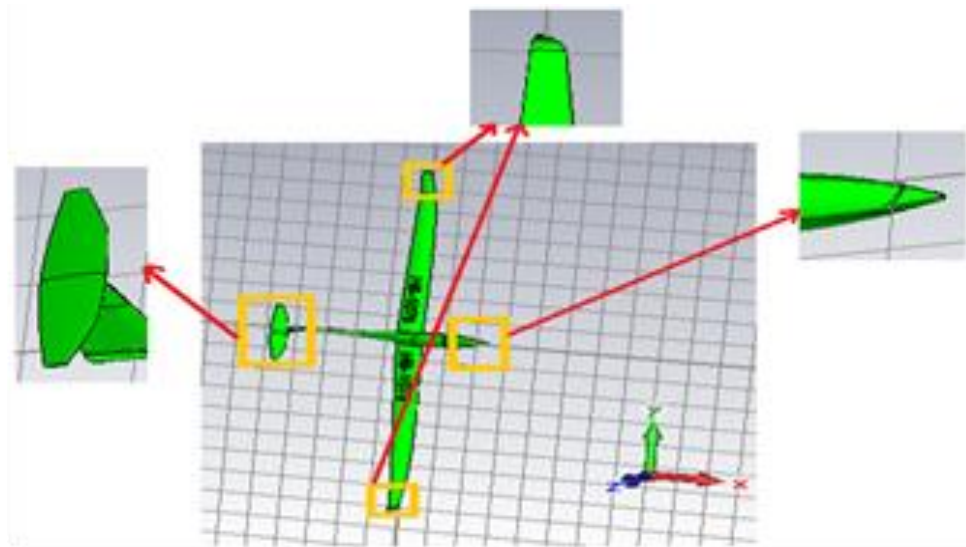


Fig. 6. Glider as a real target.

The diagram of Fig. 3 can be used to implement the above mentioned scenario. The generated raw data is used instead of radar data of target and this data can be used for data analysis, image interpretation, target recognition, and other applications. This raw data can also be used to generate signal space and image space in MATLAB software. In the simulation results section, the proposed model and CAD results are compared. The block diagram of Fig. 4 shows the image space formation.

IV. SIMULATION RESULTS

In this section, a distributed target should be taken for the implementation of the proposed algorithm, which uses a PEC-type glider. The target simulation is then done using the presented method for the glider in this article. To compare the results, the CAD model of the glider is also simulated.

The scattering matrix is one of the measurement parameters. In man-made targets, unlike natural targets, the cross-polar scattering is negligible, and this feature separates the man-made targets from natural ones [16-18]. The co-polar scattering offers features to distinguish [15]. Man-made targets are used in this study, therefore, HH polarization has been used. Characteristics of simulated SAR in the CST software are shown in Table II.

In this part, to simulate the proposed method, the scattering points related to the glider in different angles and directions will be extract at first, and then replace the extracted pixels with the canonical shapes. After that the target image space using the canonical shapes will be obtained. As Shown in Fig. 5, the imaging coordinates proportional to the spherical system are θ (incidence angle) and φ (scan angle). As mentioned above, the first step is to identify scattered pixels at the target. For example, the glider nose, wings, and the elevator of the glider are scattered pixels in the glider. Fig. 6 shows the glider scattered pixels.

In the second step, after determining the position, orientation and target shape in the scattered pixels. These pixels are replaced with similar simple models. In the proposed model, the nose of cone-shaped glider, according to its orientation will be replaced with the cone at the nose position. Also the wing and elevator which are plate-shaped, according to the orientation of target, will be replaced with plates at the wings position. The model is shown in Fig. 7.

In the following, the glider image space and the presented model at various scan angles are given. We have done three experiments with $(\theta = 90, \varphi = 0)$, $(\theta = 90, \varphi = 90)$, $(\theta = 90, \varphi = 45)$ degrees. In the first case, the glider image space at the incidence angle $\theta = 90$ degrees and the scan angle $\varphi = 0$ degrees are considered.

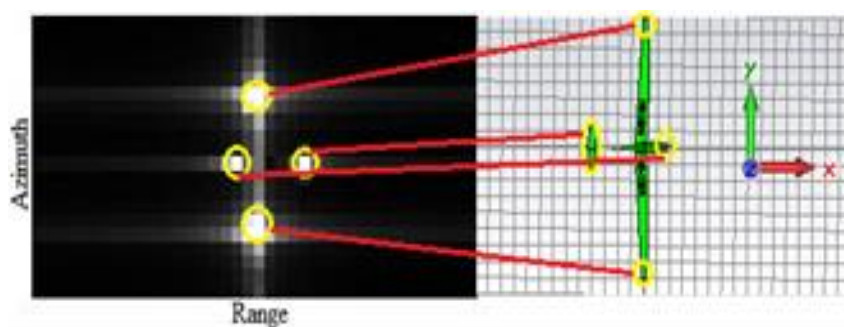


Fig. 8. The glider image space at the incidence angle $\theta = 90$ and the scan angle $\varphi = 0$

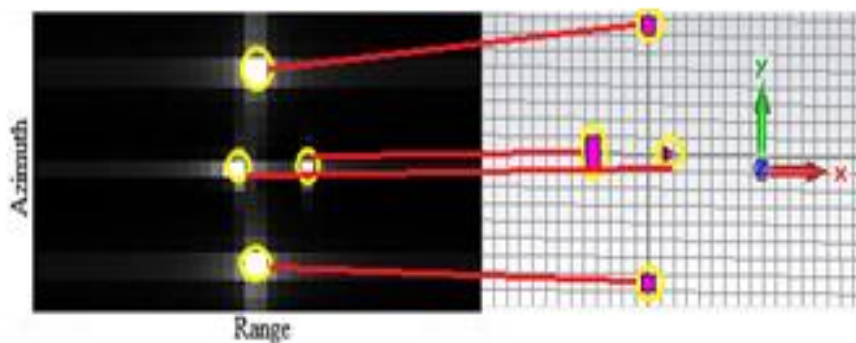


Fig. 9 . The image space of the replaced model at the incidence angle $\theta = 90$ degrees and the scan angle $\varphi = 0$ degrees

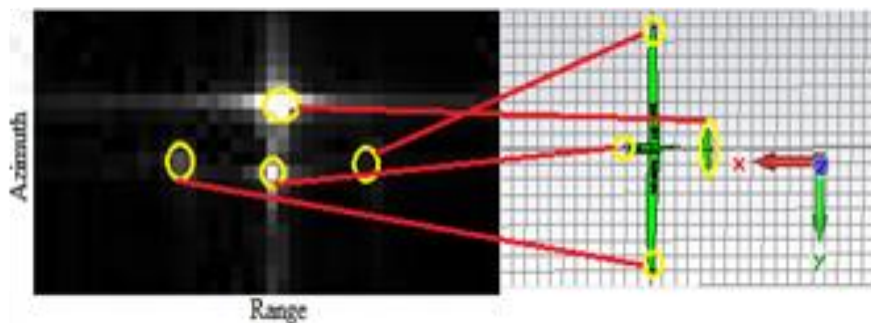


Fig. 10. The image space of the glider at the incidence angle $\theta = 90$ and the scan angle $\varphi = 90$

As seen in Fig. 8, the nose, wings and the elevator of the glider have the most scattering toward the radar. Accordingly, the image space of the replaced model at the incidence angle $\theta = 90$ degrees and the scan angle $\varphi = 0$ degrees are shown in Fig. 9.

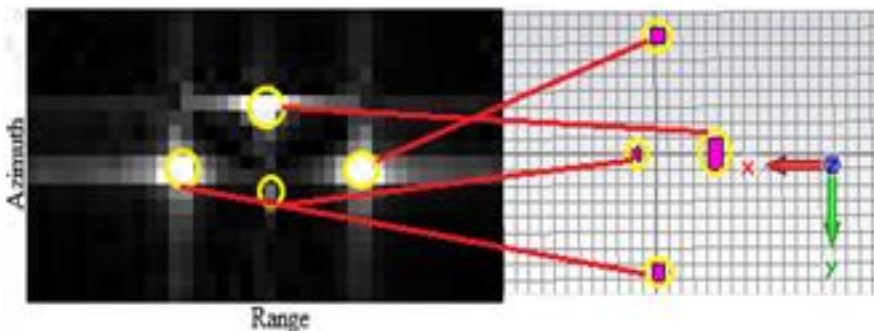


Fig. 11. The replaced model at the incidence angle $\theta = 90$ and the scan angle $\varphi = 90$.

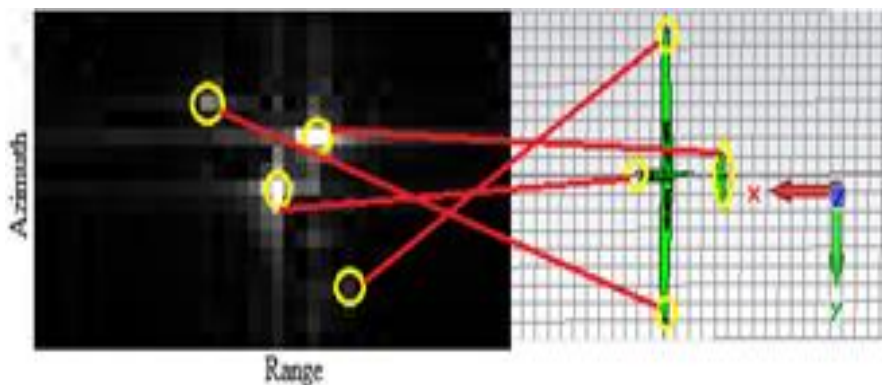


Fig. 12. The image space of the glider at the incidence angle $\theta = 90$ and the scan angle $\varphi = 45$.

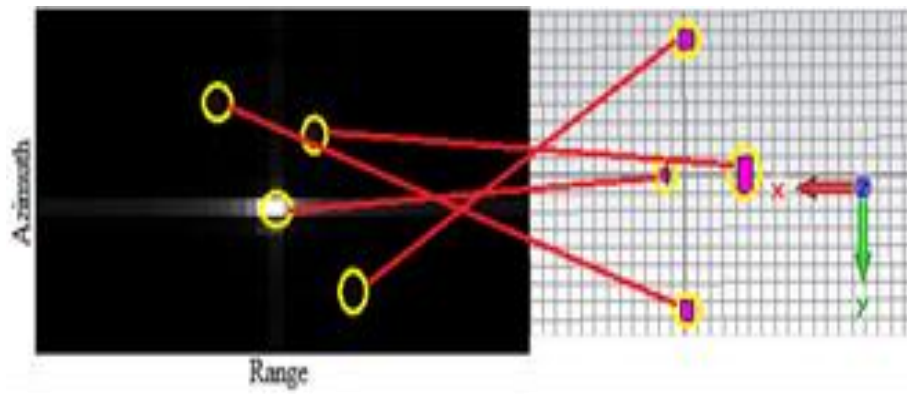


Fig. 13. The replaced model at the incidence angle $\theta = 90$ and the scan angle $\varphi = 45$.

In the second case, the image space of the glider and the replaced model are considered at $\theta = 90$ and $\varphi = 90$. The results are shown in Figs. 10 and 11. Also the results for $\theta = 90$ and $\varphi = 45$ are shown in Figs. 12 and 13.

Target Sign	Target	Replaced Model
A		
B		
C		
D		

Fig. 14. Example of the selected targets and replaced models.

The simulation results show that, as expected, the image of the glider and the replaced model have the same peak. Due to the complexity of the glider, minor differences in peak intensity and location are observed in some cases.

To compare the difference between the image space of the glider and the replaced model, the RMSE (Root Mean Square Error) criterion between the image space and the replaced model is calculated at different angles according to the following formula [14]:

$$RMSE = \sqrt{\frac{\sum_{i=1}^n (X_{1,i} - X_{2,i})^2}{n}} \quad (1)$$

Table III. RMSE for Glider image Space and replaced Model

Scan Angle	RMSE
$\varphi = 0$	0.012
$\varphi = 45$	0.0072
$\varphi = 90$	0.1327

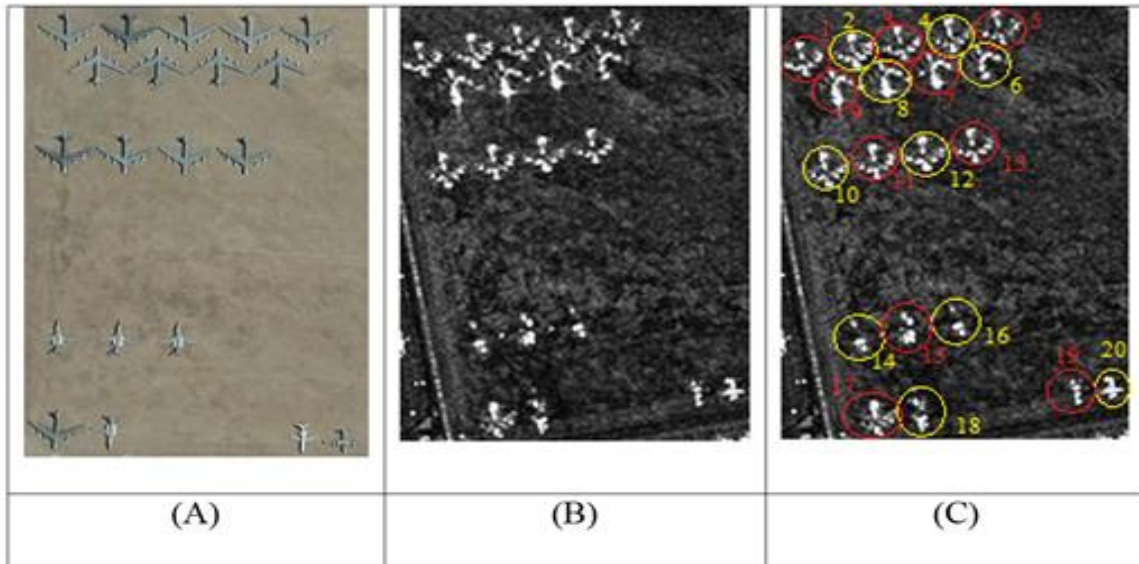


Fig. 15. (A) optical image of Tucson, AZ, USA recorded by Google Earth (B) SAR image of same region recorded by Terra SAR-X (C) targets numbering.

The RMSE results for the glider image space and the replaced model for the different scan angles are listed in Table III.

According to the calculations in the above table, the value of the RMSE is small. These results indicate the closeness of the result of the real and replaced model. As stated, one of the uses of the proposed model is the target recognition. For this purpose, four targets in the optical image are selected as terrain data and the results are used to identify targets in the Terra SAR-X image. The selected area is the Tucson, Arizona, USA with a latitude of $32^{\circ}10'27.16''N$ and a longitude of $110^{\circ}51'20.83''W$ in HH polarization on 23/12/2010. The selected targets are shown in Fig. 14.

Table IV. The results of target recognition

Number of Target	Recognized	Ground Truth
1	A	A
2	A	A
3	A	A
4	A	A
5	A	A
6	A	A
7	A	A
8	A	A
9	A	A
10	A	A
11	A	A
12	A	A
13	A	A
14	B	B
15	B	B
16	B	B
17	A	A
18	B	B
19	D	D
20	C	C

V. CONCLUSION

In this paper, a new model is presented to obtain the scattering fields of complex distributed targets. In recent years, the applications of SAR radars have increased, but the exact recognition of the target in the image is not yet possible. The proposed model makes it possible to study the features of the targets in the scene and also it provides the possibility of target detection. Identification of the target's effect based on the unique response of target is applicable in stealth technology, target recognition, categorization and analysis of targets for scattering fields. In addition, the target radar cross-section can be created by design a structure and can be used as deception in the passive defence purposes. For example, the glider is physically replaced with cones and plates. The result of this research create the following capabilities:

1. Understanding the patterns of the SAR targets allows for the interpretation of SAR images. In addition, target recognition is possible with the unique of the response.
2. The prediction of the target's scattering data causes the identification of the target. In addition, it improves target design and radar design for specific purposes.
3. Due to the importance of this system, this model can be helpful in passive defence solution to deal with this system.
4. The physical implementation of the model causes ease of implementation of the deception scheme. The idea of other executive designs is possible with this capability.

REFERENCES

- [1] P. Tait, Introduction to radar target recognition, London: The Institution of Engineering and Technology, 2009.
- [2] M. G. Kaller, Matching algorithms and feature match quality measures for model-based object recognition with applications to automatic target recognition. Mathematical Sciences Graduate School of Arts and Science, New York, 1999.
- [3] A. Schroth, K. H. Bethke, and W. Herdeg, "High resolution polarimetric radar imaging and applications," *Frequenz*, vol. 49, pp. 3-4, March 1995.
- [4] C. W. Huang, & K. C. Lee, "Frequency-diversity RCS based target recognition with ICA projection," *Journal of Electromagnetic Waves and Applications*, vol. 24, no. 17-18, pp. 2547-2559, Apr. 2010.
- [5] Sh. Liu, R. Zhan, J. Zhang, and Zh. Zhuang, "Radar automatic target recognition based on sequential vanishing component analysis," *Progress in Electromagnetics Research*, vol. 145, pp. 241-250, May. 2014.
- [6] Y. L. Chang, C. Y. Chiang, and K. S. Chen, "SAR image simulation with application to target recognition," *Progress in Electromagnetics Research*, vol. 119, pp. 35-57, Apr. 2011.
- [7] G. Cakir and L. Sevgi, "Radar cross-section (RCS) analysis of high frequency surface wave radar targets. Search Results," *Turkish Journal of Electrical Engineering Computer Sciences* , vol.18, no.3, May 2010.
- [8] P. Chen, C. Qi, L. Wu, and X. Wang, "Estimation of extended targets based on compressed sensing in cognitive radar system," *IEEE Trans. on Vehicular Technology*, vol. 66, no. 2, pp.941-951, Feb. 2017.
- [9] B. Wang, Z. Hu, W. Guan, Q. Liu, and J. Guo, "Study on the echo signal model and R-D imaging algorithm for FMCW SAR," *IET International. Radar Conference*, pp. 1-6, Oct. 2015.
- [10] I. G. Cumming and F. H. Wong, Digital processing of synthetic aperture radar data. London: Artech House, 2005.
- [11] J. A. Richards, Remote sensing with imaging radar. New York, NY: Springer, 2009.
- [12] C. V. Jakowatz, D. E. Whal, P. H. Eichel, D. C. Ghiglia, and P. A. Thompson, Spotlight-mode synthetic aperture radar: A signal processing approach. London: Kluwer Academic Publishers, 1996.
- [13] W. L. Melvin, & J. A. Scheer, Principles of modern radar. SciTech Publishing, 2013.
- [14] M. B. Fallahpour, H. Dehghani, A. J. Rashidi, and A. Sheikhi, "Analytical modelling and software implementation of Synthetic Aperture Radars. International Journal of Electronics," vol. 104, no. 11, pp. 1795-1809, May 2017.
- [15] M. B. Fallahpour, H. Dehghani, A. J. Rashidi, and A. Sheikhi, "SAR target recognition using behaviour library of different shapes in different incidence angles and polarizations," *Intern. Journal of Electronics*, pp. 771-783, Nov. 2017.
- [16] A. Vyas and B. Sashtri, "SAR polarimetric signatures for urban targets. polarimetric signature calculation and visualization," *International Archives of the Photogrammetry, Remote Sensing and Spatial Information Sciences*, Aug. 2012. doi.org/10.5194/isprsarchives-XXXIX-B7-535-2012
- [17] M. Nord, T. L. Ainsworth, J. S. Lee, and N. Stacy, "Comparison of compact polarimetric synthetic aperture radar modes," *IEEE Trans. on Geoscience and Remote Sensing*, 47, no. 1, pp. 174 – 188, Jan. 2009.
- [18] T. Moriyama, S. Uratsuka, K. Nakamura, and T. Umehara, "Polarimetric SAR image analysis using model fit for urban structure," *IEICE Trans. on Communications*, vol. 47, pp. 174-188, Jan. 2005..